DIFFUSED QUANTUM WELL STRUCTURES : ADVANCES IN MATERIALS AND DEVICE REALIZATIONS

E. HERBERT LI
Department of Electrical and Electronic Engineering,
University of Hong Kong, Pokfulam Road, Hong Kong.
Email : ehli@eee.hku.hk

ABSTRACT

The Diffused Quantum Well (DFQW) structures created by both impurity induced and impurity free or vacancy promoted processes have recently been advanced to a higher level. The interdiffusion mechanism is no longer confined to two constituent atoms, but consists of two or multiple phase interdiffusion as well as multiple species, such as three cations interdiffusion and two pairs of cation-anion interdiffusion. Results show that the outcome of these interdiffusions is quite different. For instance, both compressive or tensile strain materials and both blue or red shifts in the bandgap can be achieved dependent on the type of interdiffusion. The advantage of being able to tune the material properties allows the realizations of higher performance lasers and modulators. Two lasing wavelengths (60 nm apart) are produced at $\lambda \approx 1.55\mu m$, on the same substrate, with threshold currents of 290mA, and an extremely large relative reflectance change (over 10000) is predicted with power consumption reduced by 67%. A six fold enhancement of the third order susceptibility over that of the bulk materials can be achieved by using the inter-subband transitions in the DFQW at $\lambda \approx 10\mu m$. Broadband (1000nm) detectors have also been realized due to the wide DFQW spectral bandwidth. Several state-of-the-art results of the DFQW will be summarized with an emphasis on the future developments and directions of the DFQW.

INTRODUCTION

Diffused quantum well (DFQW) is a non-square quantum well produced by interdiffusion of constituent atoms through the heterointerface. In the literature, DFQW is also referred to as quantum well mixing or intermixing (QWI) and quantum well disordering. Extensive work has recently been focused on the application of DFQWs since they provide post-growth tuning of the device operating wavelengths. The DFQWs can also be produced by a controlled interdiffusion process, which allows the rate of diffusion to be varied. This enables a selective area quantum well intermixing technology to laterally confine light for waveguiding. The process of achieving optical lateral confinement includes impurity induced disordering (IID) and impurity-free vacancy diffusion (IFVD). Performance of devices using DFQWs can also be improved and contribute to easy and effective realization of photonic integrated circuits.

The first work [1] on DFQW reported that Zn diffusion into an AlAs-GaAs superlatice, or into $Al_xGa_{1-x}As$-GaAs quantum well heterostructures can enhance the Al-Ga interdiffusion rate at the heterointerfaces and create uniform compositionally disordered $Al_xGa_{1-x}As$ even at lower temperature. Following this, the disk-shaped IR-red GaAs-AlAs superlattice lasers were demonstrated (cw 300K), which were monolithically integrated into rectangular yellow-gap $Al_xGa_{1-x}As$ cavities [2]. This process had become a first patent base on QW mixing.

In recent years, great effort has been put in using DFQW as a tool. Last year, several remarkable papers on lasers and modulators using DFQWs were published. For instance, the fabrication of multiple wavelength lasers and mutli-channel wavelength division multiplexers in GaAs/AlGaAs structures have been achieved using the technique of "selective intermixing in selected area" (SISA), based on IFVD [3]. Buried InGaAs/InP quantum wires with width down to 15mm was fabricated by lateral barrier modulation. The key technique involved was the local removal of the InP top barrier layer of the QW using high resolution electron beam lithography and selective wet chemical etching [4]. Impurity-free

Mat. Res. Soc. Symp. Proc. Vol. 450 © 1997 Materials Research Society

disordering of InP based InGaAs/InGaAlAs QWs induced by three different dielectric thin cap films (SiO_2, SiN_x, SrF_2) has been produced [5]. Detail investigation of the in-plane spatial resolution of the disordering process was also developed [5]. In fact, significant reduction of threshold currents by IID in InGaAs/GaAs QW Ridge-Waveguide Lasers has succeeded [6]. Vertical cavity surface emitting lasers employing a Zn diffused and disordered spatial mode filter were fabricated and tested [61]. Low divergence output beam of surface emission was yielded and it is suitable for short haul optical fiber. Another device which is of interest is the superluminescent diode [8] whose band emission spectrum is broad enough for high sensitivity in fiber optical gyroscopes. In addition, report of reviews have been made on IID by Holonyak in 1988 [9], on the process of DFQW optoelectronics by Weiss in 1990 [10], and on QWI by Marsh in 1993 [11].

In this paper, we aim to make a comprehensive summary on the latest progress and development in DFQWs in different areas ranging from materials, production techniques, diffusion mechanisms, to device applications.

TECHNIQUES FOR MODIFYING INTERDIFFUSION RATES IN QWs

Ion Implantation

Ion Implantation is a technique in which direct injection of ionized, energetic atoms or molecules into a solid is employed. The ions injected will carry energies ranging from a few keV to several MeV, and implant doses from 10^{10} to more than 10^{16} ions/cm^2. Using small implantation energy, the damage introduced to the lattice structure will be reduced but with a decrease in the penetration depth, while with small dose of implants, there will be lesser enhancement of diffusion rate.

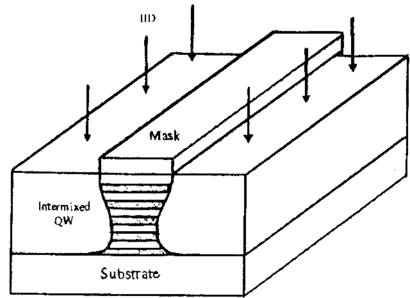

Fig. 1

Ion Implantation will significantly enhance the interdiffusion rate, and control the lateral and vertical depth of diffusion precisely (see Fig. 1). Different combinations of ions and substrates are possible and the most commonly used ones are p-type ions (Zn, Be), n-type ions (Si), neutral type ions (O), and constituent ions (Al, Ga, As) in AlGaAs/GaAs. It was reported that the use of neutral ions (including constituent ions) can prevent the production of free carriers induced by the charged ions (n-type or p-type) which will introduce propagation loss and thus reduce the refractive index of the intermixed QW materials [49]. Recent application of different implants are discussed as follows.

Interdiffusion of Al-Ga in an $Al_{0.3}Ga_{0.7}As$/GaAs supperlattice with focused-ion-beam implantation using Si has recently been studied [12]. This implantation technique provides maskless process with high spatial resolution and so, it enables precise patterning on the wafer for optoelectronics integrated circuits (OEIC) applications. Si ions are accelerated to 50 and 100 keV, and with rapid thermal annealing (RTA) at 950 ^{0}C for 10s. The diffusion coefficient was extracted to be 4.5×10^{-14}cm^2/s (with a Si ion dose of 1×10^{14}/cm^2) and in comparison with RTA, which can only produce an interdiffusion coefficient of 1.3×10^{-16} cm^2/s. This implies a 2 order magnitude enhancement.

In terms of constituent implantation, implanted gallium into both GaAs/AlGaAs and InGaAs/GaAs QWs have been performed and no significant effect on the diffusion coefficients was found in either systems. For arsenic implantation, the GaAs/AlGaAs system behaved identically to the Ga implanted sample, while in InGaAs/GaAs a region of enhanced interdiffusion was found, where the diffusion coefficient was enhanced by one order of magnitude [13].

Photoluminescence of low-energy, low dose oxygen ion implantation into AlGaAs/GaAs QWs has been studied [14]. Results showed that significant intermixing of both single and multiple

AlGaAs/GaAs QWs has been achieved using 155 keV implantation energy with doses as small as 5 x 10^{13} cm^{-2} after a moderate annealing step. A PL peak shift of 139 meV was observed in a 100Å GaAs QW after implanting 10^{14} cm^{-2} oxygen ions at 155 keV and annealed at 1050 °C for 40s, while a shift of up to 100 meV was obtained in the MQW with a dose of 8 x 10^{14} cm^{-2} ions at 450 keV with annealing at 950 °C for 120s.

In spite of these advantages, however, ion implantation technique will introduce more lattice damage and a large amount of defects in the materials. In order to reduce lattice damages, implantation energy is limited and thus, the penetration depth will be reduced.

Impurity Diffusion with Rapid Thermal Annealing

RTA is an essential step in impurity diffusion. Since impurity diffusion process undergoes a very slow rate on its own at conventional conditions, RTA is therefore used to promote its diffusion rate. RTA under temperature ranging from 900 to 1125 °C leads to substantial increase in interdiffusion rate. Most of the annealing is usually performed in the range from 400 to 1000 °C, and under a chemical environment with N_2 or even in vacuum to prevent oxidation to occur.

Marsh has demonstrated a method of RTA [11], in which flourine-implanted SCH and GRIN samples were capped with 1000Å of either SiO_2 or Si_3N_4 deposited by plasma-enhanced chemical vapour deposition. RTA is then performed at different temperatures (650 to 750 °C) in a nitrogen atmosphere. A more recent RTA experiment was performed in 1996 by Bacher which consists of samples annealed for one minute between 450 and 750 °C under a continuous flux of nitrogen to avoid surface oxidation [15].

Recently, there is a report on an novel application of impurity diffusion [50]. The structure used is a 80-period GaAs/AlAs superlattice with each layer 34 Å thick, Si dopped and annealed at 800 °C with a carbon source for 3 hours. PL spectra showed that the magnitude of the intermixing of Al and Ga increases with depth which is in contrast with the intermixing mechanism considering vacancy injection from the surface. This is because in theory, the diffusion coefficient of carbon is very small and hence carbon remains mainly at the surface of the MQW. Reduction of Si diffusion speed is mainly due to the combination of Si and carbon. As a result, the intermixing coefficient is small at the surface and increase gradually with depth.

In general, flexibility of easy alteration of the compositional profile inside the material is made possible in impurity diffusion. However, unintentional intermixing may take place in regions other than those implanted and precise depth control cannot be achieved with this diffusion method. The volume concentration of impurity drops during interdiffusion and will eventually drop below the threshold concentration at which the implantation enhanced disordering occurs.

Impurity Free Vacancy Diffusion (IFVD)

The mechanism of IFVD requires the encapsulation of MQW samples by a dielectric cap such as SiO_2 or Si_3N_4 (see Fig. 2) and then annealing at high temperature around 850 °C ~ 900 °C for 30 to 180 seconds. This will lead to out-diffusion of Ga into the cap and vacancies are generated on the group III sublattice that diffuse to the barriers and promote the interdiffusion in the MQWs. By using different combination of caps, selective area bandgap control is possible.

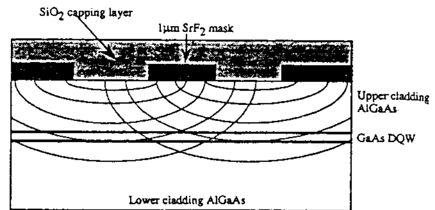

Fig. 2 [3]

A recent experiment on IFVD [16] was performed to investigate whether Ga vacancy are generated during SiO_2 capping and annealing. A uniformly Si doped GaAs epilayer of 10um thick with n = 4.8 x 10^{18} cm^{-3} grown by MBE was studied using photoluminscence and cathodoluminescence. As a

result, an increase in the strength of the emission at 1.2 eV is observed which is attributed to the Ga vacancy. This evidence shown that Ga vacancy is the species responsible for IFVD.

The advantage of using IFVD is that it is a simple method which requires much less equipment to perform. As discussed above in using ion implantation, only neutral species IID can circumvent the large optical propagation losses associated. However, neutral impurities still introduce substantial changes in material resistivity and trap concentrations. IFVD can create large bandgap energy shifts without these disadvantages of IID. However, using IFVD will increase the number of etching steps needed to control the thickness of SiO_2. Moreover, control of oxygen composition in SiO_xN_y is complex.

Laser Assisted Disordering

Laser assisted disordering is a direct write process that can pattern impurity induced layer disordering. This new technique employs a highly focused Ar^+ laser beam (see Fig. 3). For fabrication of AlGaAs-GaAs DFQW [17], the laser beam with lasing wavelength of 488 nm, is scanned through the heterostructure sample which is encapsulated with a 90 nm layer of $Si\text{-}Si_3N_4$. Its scan speed can be as high as 85 μm/s. The laser beam interaction region will result in a smooth cylindrical section on the micron scale. Annealing is then applied to drive the Si into the as-grown crystal, resulting in a local mixing of the crystal layers.

In a more recent report, pulsed photoabsorption-induced disordering technique was used to seleetively intermix GaInAs/GaInAsP QW structure, which was studied by the use of high spatial resolution time-resolved PL. Measurements showed that a reduction in the non-radioactive recombination time of nearly two orders of magnitude as a result of this intermixing technique [53].

The laser assisted technique is a flexible process for optoelectronic device and circuit fabrication. However, a direct-write system is not an optium configuration for many application. For example, commercial production of diode lasers is based upon high yield, high throughput techniques such as photolighography. Further improvement is required.

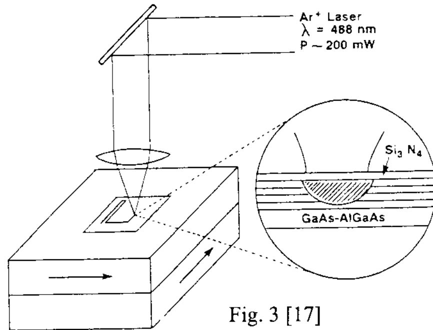

Fig. 3 [17]

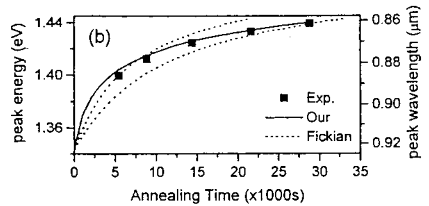

Fig. 4 [19]

DIFFUSION MECHANISM

One Phase, Group III in $A_xB_{1-x}C$ system

Simple calculations were made under Fick's Law of diffusion to determine the composition profile x(z) for $Al_xGa_{1-x}As/GaAs$ and $In_xGa_{1-x}As/GaAs$ QWs [18]. This simple model leads to error function solutions :

$$x(z) = x_0\left\{R_1 - \frac{1}{2}R_1\left[\mathrm{erf}\left(\frac{L_z + 2z}{4L_d}\right) + \mathrm{erf}\left(\frac{L_z - 2z}{4L_d}\right)\right]\right\}$$

where z is the growth axis, x_0 is the as-grown composition of the QW material, L_D is the interdiffusion length and L_z is the well thickness. For AlGaAs/GaAs QW, $R_1 = R_2 = 1$ and for InGaAs/GaAs QW, $R_1 = 0$

& $R_2 = -1$. It has been reported that this equation accounts for a wide range of diffusion coefficient values obtained in various III-V semiconductor systems [51,52].

On the other hand, it has been found recently that the above Fick's diffusion equation may not properly describe the interdiffsuion in the InGaAs/GaAs QW with strain [19]. The strain is believed to introduce changes in crystal defect concentration and thus diffusivity is also influenced by strain. Therefore, the non-Fickian equation, which is an expanded form of Fick's second law, is introduced :

$$\frac{\partial C}{\partial t} = \frac{\partial}{\partial z}\left(D_0 \exp(\kappa\ C) \frac{\partial C}{\partial z} \right)$$

where C is the indium concentration, D_0 is the diffusivity when no stress is applied, κ is the parameter indicating the degree of strain enhancement and is also a function of In concentration.

This equation has included the effects of strains empirically. The experimental PL peak shifts as a function of annealing time were well fitted by this equation, as shown in Fig. 4. Useful parameters, such as diffusivity of InGaAs/GaAs QW were found using this equation.

One Phase, Group III only in $A_xB_{1-x}C_yD_{1-y}$

Cation interdiffusion results in the formation of an InGaP/InGaAs abrupt interface from as-grown InGaAs/InP QW. Theoretical analysis [25] indicates that a large strain was built up across the well during early stage of interdiffusion. The strain and its effect on the bandgap profile of the disordered structure produces a distinctive quantum confinement profile which remains abrupt even after significant interdiffusion. This phenomenon together with a diffused well width which equals to that of the as-grown QW are in contrast to other material systems such as AlGaAs/GaAs and InGaAs/GaAs. The effect of strain results in a potential buildup in the barrier near the interface at the top of the well, while it gives rise to two miniwells at the bottom of the wells. The HH and LH band-edge splitting results in two distinct HH and LH confinement profiles with different depths.

One Phase, Group III plus V in $A_xB_{1-x}C_yD_{1-y}$ system

The effect of interdiffusion on the confinement profile of the quaternary material systems has been reported recently [20]. The intermixing of $In_{0.53}Ga_{0.47}As$/InP has been modeled, taking into account different interdiffusion rates on the group III and group V sublattice. Error function distribution discussed above was used to represent the composition profile. A strained QW was resulted after intermixing. Theoretical results showed that when the cation interdiffusion rate is faster than that of the anion, the ground-state (C1-HH1) transition shifts to longer wavelengths. For prolonged interdiffusion, this shift to longer wavelengths, saturates and then decreases. This is in good agreement with the reported experimental results of Zn-diffused disordering [21-23] as well as thermal annealing of InGaAs/InP QWs [24]. When the anion diffusion rate is faster, results showed that the effective bandgap of the diffused QW would be the C1-LH1 ground state transition which shifts to shorter wavelength with interdiffusion. The tensile strain that is induced under these disordering conditions which moves the LH ground state above the HH ground state. Results obtained from these calculations showed that the control of relative extent of cation and anion interdiffusion offers different possiblities for optoelectronic device fabrication.

Two Phase, Group V in $A_xB_{1-x}C_yD_{1-y}$ system

Mukai [26] has derived a formula that describes the two-phase interdiffusion mechanism of the quaternary material system which includes the different interdiffusion coefficients between layers and interfacial discontinuity of interdiffused species. The formula was applied to analyze the dependence of an interdiffusion induced energy shift on annealing time, annealing temperature and well width in InGaAsP/InP QWs. Good agreement was achieved between the calculated and measured values.

Two phase Group V sublattice interdiffusion in $In_{0.53}Ga_{0.47}As$/InP QW was also theoretically investigated [27] using the same formulation with a pseudo time dependence. This model has been

validated with an even better agreement with experimental results. However, perfect fitting can not be obtained and further work must be continued.

Multiple Species, Group III

The most recent analysis on multiple cations interdiffusion in $In_{0.53}Ga_{0.47}As/In_{0.52}Al_{0.48}As$ is performed using a model base on the expanded form of Fick's second law [28]:

$$\frac{\partial C_i}{\partial t} = \sum_{j=1}^{n-1} D_{ij} \nabla^2 C_{ij}$$

where n = the number of diffusable species, C is the indium concentration, D_0 is the diffusivity when no stress is applied. The model is fitted to the measured concentration data in order to determine their diffusion coefficients. It was found that the Ga-Ga diffusion coefficient is relatively large in comparison to the other rates so that the Ga concentration profiles show a more broadened distribution after annealing (see Fig. 5). The In-Ga diffusion is fund to be negative which gives rise to the inverse process of diffusion, causes sudden abrupt change in the In profiles at the interfaces. Again, further experimental work should be done to enable a large set of data to be fully analyzed.

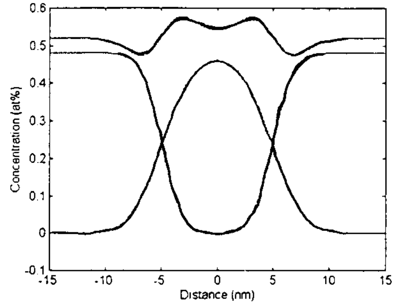

Fig. 5

BAND STRUCTURE

Effects of interdiffusion on the subbands in an AlGaAs/GaAs QW has been investigated theoretically [29] in which the subband energies and wave functions in an interdiffusion-induced AlGaAs/GaAs single quantum well structure were calculated. The confinement profile was modeled by an error function. The spatially dependent electron effective mass was taken into consideration using a non-parabolic band model derived from a fourth-order expansion in k with the coefficients determined using a 14-band calculation. The valence subband mixing between the heavy and light holes were also considered. It was found that subband properties of the nonsquare QW was different from that of the conventional SQW. First of all, the subband-edge energy will initially increase and then decrease with interdiffusion, which could be explained by the evolution of the nonsquare QW shape in terms of crossover point, which is defined as the confinement profile intersection at the well barrier interface of the as-grown and interdiffused QWs. Enhancement of interband transition is predicted for the off-diagonal selection rule at the initial stages of interdiffusion, and a reduced confinement of the wave function was also observed. Lastly, the enhancement of the lowest energy light-hole negative mass was also obtained. The non-monotonic behavior of the subband-edge energies suggested hat when only the lowest interband energy was used to characterize the interdiffusion process, errors are likely to occur. Analysis has also been done on InGaAs/GaAs QW and InGaAs/InP QW structures [30,31].

FAR-IR OPTICAL PROPERTIES

The first theoretical study of the linear and nonlinear intersubband absorption coefficients in AlGaAs/GaAs DFQW was reported by Li [59] following the first observation of an interdiffusion shifted intersubband transition energy by Ralston [60], see Fig. 6. Results indicated that the well shape variation can provide a large tuning wavelength range in the far IR region with an almost constant absorption. This DFQW structure can be used to produce a wide bandwidth detector. The DFQW structure can also provide lower leakage currents due to reduced tunneling between the wells since the barrier thickness at the ground state energy is always thicker than that at the excited state energy. Effects of interdiffusion on the intersubband optical properties in a modulated doped QW structure have also been investigated

theoretically [32]. Linear and nonlinear intersubband electroabsorption and the change in refractive index with different well width, doping concentration, Aluminium concentration ration in AlGaAs/GaAs QW were studied. A wide tuning range has been predicted which can be applied to the realization of multi-color and broadband photodetector. More recently, a DFQW has been employed to predict the enhancement of the third-harmonic susceptibility to an extent that it is six times better than the case of GaAs [33]. The obtained $\chi^{(3)}$ enhancement is as high as 2700 $(nm/V)^2$, as shown in Fig. 7, and may also be carefully varied to produce a tuning range. However, there are still technical problems in fabricating with a high yield and low price.

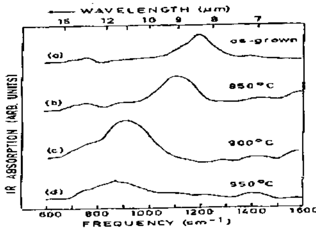

Fig. 6 [60]

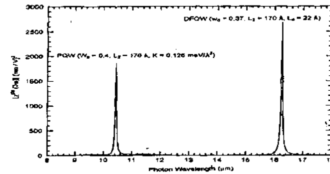

Fig. 7 [33]

Fig. 6 and 7 show the enhancement of $\chi^{(3)}$ in which shifting of intersubband absorption resonance occurs.

INTER-BAND IR OPTICAL PROPERTIES

Absorption

The most recent experimental work of partially intermixed QW waveguides is performed in 1989 [34], with the incident focused laser beam polarized both parallel (TE) and perpendicular (TM) to the plane of the QW layers. These spectra show the polarization anisotropy characteristic of QW absorption. In the TE spectra, both the lh and hh excitons appear while in the TM spectra, the hh exciton disappears and the lh exciton absorption strength increases. The intermixing induced band-edge shifts are clearly seen. There are theoretical studies in which a hyperbolic function has been used to model the confinement profile of a disordered $Al_{0.3}Ga_{0.7}As$/GaAs QW [54] and results predict a different absorption spectra for the TE and TM polarization, and which is in good agreement with published measurements near the absorption edge. In a more recent investigation, theoretical calculations are performed on polarized absorption coefficients of interdiffused AlGaAs/GaAs MQW [55]. Calculations were made without any approximation or presumption of the eigenstates. Results showed that for diffusion length ranging from 10Å to 30Å, the blue shift of the absorption edge is larger. The two dimensional QW properties were strongest in the beginning of interdiffusion.

Refractive Index

The effect of boron and fluorine IID on n_R of AlGaAs MQW was studied experimentally [39]. Substantial changes of > 1% in the refractive index were obtained in partially disordered material over the measured wavelength range. This implies that fluorine produces larger change than boron for similar annealing conditions. A few years later, experiment has been performed to investigate the effect of Zn IID on the refractive of AlGaAs/GaAs MQWs [38]. This is a structure consisting of several uncoupled MQW ridge waveguides with tapered disordering across the transverse direction was employed. The refractive index changes have been deduced as a function of the Ga/Al interdiffusion length by the use of an interference technique. A maximum index change of 0.083 and 0.062 was measured for significant disordering (L_d = 6.6 nm) at 35 and 100 meV below the band edge energy of the as-grown MQW respectively.

Moreover, the polarization dependent refractive index for both $Al_{0.3}Ga_{0.7}As/GaAs$ and $In_{0.2}Ga_{0.8}As/GaAs$ single QWs are calculated [36,37]. The confinement profile for the $Al_{0.3}Ga_{0.7}As/GaAs$ DFQW is modeled by an error function and n_R is determined by the real and imaginary parts of the dielectric function including contributions from the Γ, X and L Brillouin zones. It was found that at longer wavelengths, n_R decreases with increasing interdiffusion which normally provides a positive index step with respect to a less interdiffused QW. For shorter wavelengths, the wavelength range for a positive refractive index step increases as the extent of disordering between two interdiffused QWs is increasing. Polarization dependent n_R of disordered, strained InGaAs/GaAs single QWs was also calculated using the same method applied to $Al_{0.3}Ga_{0.7}As/GaAs$ QW. In this calculation, decrease in refractive index with increase in the extent of disordering at longer wavelengths was observed. These structures also exhibit birefringence in a range of wavelengths from the QW band-edge to barrier band-edge, which decreases with interdiffusion.

Electro-absorption and Electro-Optic

There has been one experimental measurement on perpendicular field electroabsorption in GaAs/AlGaAs QW structures [34] which have been modified via partial interdiffusion of the well and barrier layers. Quantum well Stark effect has been observed in the DFQW where the room temperature exciton peaks are blue shifted by at least 40 meV via partial layer interdiffusion. On the other hand, the Quantum well Stark effect has also been analyzed theoretically in an AlGaAs/GaAs DFQW. Results showed a twofold enhancement of the Stark shift for the interdiffused QW over that of the square QW for the same 50 kV/cm applied field [56]. Excitonic absorption peak also shows a much larger reduction with increasing applied field in the more extensively DFQWs. These characteristics may be used to realize optical modulators with high on/off ratio and lower drive voltage.

In 1995, electric field induced refractive index change and absorption coefficient change in TE polarization are analyzed at room temperature for various interdiffusion modified $Al_{0.3}Ga_{0.7}As/GaAs$ QWs was also studied [35]. For small and medium interdiffusion lengths with fields of 100 and 50 kV/cm, respectively, improved chirping and electroabsorption can be obtained. In addition, in a selected set of interdiffusion lengths and fields, the material can be used for an electroabsorption modulator with reduced chirping in a wide range of operation wavelengths.

Optical Gain

Analyses are performed on laser gain and current density at room temperature for intermixed $Al_{0.3}Ga_{0.7}As/GaAs$ single quantum well structures [41]. It was observed that small amount of intermixing will not affect the lasing quality much. Both the peak gain and current density remain about the same strength. However, for larger amount of intermixing, the lasing will diminish. A wide wavelength tuning range of 55 nm can be obtained without greatly affecting the quality of the lasing properties. Application of selective disordering to integrated optoelectronics devices on a planar substrate can be achieved.

DEVICES

Distributed Feedback (DFB) Lasers

The realization of gain coupled DFB lasers using the method of masked implantation induced QW intermixing was demonstrated [57]. The combination of Electron Beam Lithography and the implantation enhanced intermixing was successfully applied in the fabrication. It was found that the GaInAs/AlGaInAs material system has a high potential for tunable optoelectronic devices. A detail investigation on the integration processing steps such as implantation, subsequent annealing and re-growth with InP (MOVCD) was presented. Enhancement of side mode suppression ratio (SMSR) in $\lambda/4$ shifted DFB laser using DFQW is also proposed (Fig. 6). The suppression ratio can be increased significantly by introducing diffusion step along longitudinal direction of QW active region. Results

show that large κL (>2.6) devices with step refractive index profile will exhibit stable, single-mode operation. The maximum power for single mode operation is obtained for >50 mW [42].

Vertical-cavity surface-emitting lasers (VCSEL)

In the past two years the performance of VCSELs has dramatically improved. Following the discovery of using IID for carrier confinement in edge-emitting lasers, recently, there is an investigation on the dielectic-apertured VCL structure (see Fig. 8) using Zn IID to modify the perimeter of the QW active region for achieving enhanced carrier confinement [7].

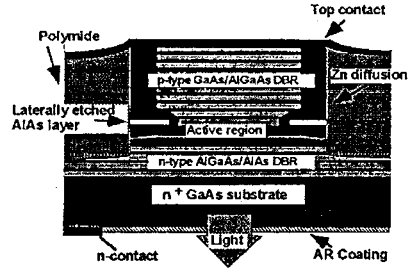

Fig. 8 [7]

The laser is tested and it was found that threshold currents as low as 0.67 mA is obtained for IID-defined VCLs. The performance of IID-VCLs has been compared to air-gap apertured VCLs fabricated from adjacent material from the same wafer. SEM images of the active region and near field EL measurements indicated that the Zn-IID has resulted in confinement of the carriers in the lasers and such confinement should enable the generation of smaller diameter VCLs in the future.

Fabry-Perot Lasers

A multiple wavelength Fabry-Perot Laser was fabricated by vacancy enhanced QW disordering which involves the use of a dielectric cap annealing. The device structure consists of a Si doped GaAs substrate, followed by a 1.1 μm thick large gap $Al_{0.8}Ga_{0.2}As$ cladding layer and a 165 nm small gap $Al_{0.3}Ga_{0.7}As$ core containing single GaAs QW (7nm). Lasing wavelength was selectively shifted by 20nm compared with fabrication by as-grown material. SrF_2 capped laser will consume 14 mA but only 10 mA for SiO_2 capped laser [43]. Theoretical analysis was also performed in which Fabry Perot semiconductor laser with periodic change in the extent of interdiffusion along the longitudinal direction of the Quantum Well active region is proposed to improve the discrimination between cavity modes [58].

IID Ridge-waveguide (RW) Lasers

Si-induced disordering is used in producing the InGaAs/GaAs QW ridge-waveguide lasers via lateral confinement. The ridge stripe is etched by pure Cl_2 plasma to form a ridge stripe. Zn diffusion is processed at 620 °C for 20 minutes. Threshold current as low as 0.7 mA for pulsed operation and 0.9 mA for cw operation was achieved. Comparing with the IID RW laser with conventional ones, great improvement in internal loss can be seen although there is a reduction of the internal quantum efficiency with respect to the conventional ones. Leakage current and threshold current for IID RW are both lower than that of conventional RW laser [6].

Vertical-cavity Fabry-Perot reflection modulator

A Fabry-Perot reflection type modulator which uses interdiffused AlGaAs/GaAs quantum wells as the active cavity material has been studied and optimized theoretically [44]. An asymmetric Bragg reflector structure (modeled by transfer matrices), with a doped depletion layer in the heterostructure, has been considered. This is the first study to model such material system in this type of modulator, and the results show improvement in modulation property over the conventional rectangular quantum well modulator. In particular, the change of reflectance in the diffused quantum well modulator is almost 0.6 to 0.7, which is higher than that of the typically available values (~0.4 to 0.6), while the OFF-state on-resonance reflectance is almost close to zero. The operation voltage is also reduced by more than half, due to a higher tunneling rate of electrons, in the large extensively diffused quantum wells. The finesse of the more extensively diffused quantum well also improves. Both of these features improve the change

of the reflectance in the modulator. The operation wavelengths can be adjusted over a range of 100nm. However, the absorption coefficient change of the diffused quantum well increases only when there is a small amount of interdiffusion.

Superluminescent Diodes

A broad-spectrum LED was fabricated by high-energy ion implantation (1MeV P^+-ions) using a SiO_2 mask (a few micron of thickness) [8]. Annealing is then performed at 700 ^{0}C for 90 seconds. The device (Fig. 9) is then etched into a ridged structure to improve guiding. An increase in the emission full-width-half-maximum from 28 nm to 90 nm was observed. Emitted power of the diode will increase with the current.

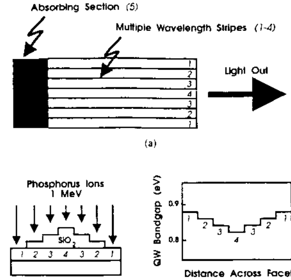

Fig. 9 [8]

Waveguide

In 1994, a novel waveguide polarization mode splitter using refractive index changes induced by superlattice disordering has been produced [45]. The operation principle of this splitter is based on the polarization-dependent refractive index changes induced by disordering InGaAs/InP sulerlattices using Si_3N_4 cap-annealing method. One attractive feature of this slpitter is that it requires no electrical control and is suitable for semiconductor monolithic integrated circuits. In 1995, a report [46] on an InGaAs/InP QW waveguide which is intermixed by using MeV phosphorous ion implantation. The bandgap is blue shifted by 90 nm in all planar process.

Infrared Photodetector

The barrier layer and well of an infrared photodetector are partially intermixed and peak detection wavelength is red shifted [47]. Successive annealing at 850 ^{0}C were used to tune the 8.13μm detector to 9.13 μm continuously. The layer structure is grown by MBE on semi-insulating GaAs substrate. Each of the 32 periods of QW consists of 346Å AlGaAs barriers and 58Å GaAs well. The peak absorption strength reduces with increasing annealing time fom 6% to 4%, but the overall quantum efficiency remains steady. The increase in dark current is mainly due to the details of subband energies and diffusion of Si through the layer structure can lower the device resistivity. The peak detection wavelength of the DFQW detector is beyond the half maximum point of that of the as-grown QW device. This indicates a clear-cut band-gap tuning between the two structures without crosstalk noise. The modified detector has responsivity comparable to as-grown material with larger spectral linewidth.

There is also a theoretical analysis of the intersubband infrared photodector performance for various stages of interdiffusion in AlGaAs/GaAs QW [40]. It was found that the absorption strength and responsivity are enhanced for certain extents of interdiffusion and the peak detection wavelength red shifts continuously with a large tunable range from 7 to 38.4 um. The dark current is at an acceptable value for small diffusion extent.

Solar Cell

Enhancement of energy conversion efficiency and spectral response by using interdiffused III-V semiconductor QW in photovoltaic device is proposed (see Fig.10). Calculations were based on an ideal solar cell model. The spectral response and energy efficiency are enhanced significantly by the DFQW structure.

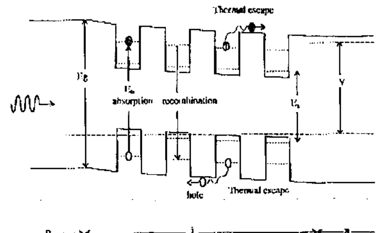

Fig. 10 [48]

Therefore, in view of the advances in the MBE and MOCVD growth techniques, DFQW photovoltaic device could provide a new approach to the high efficiency solar cell [48].

CONCLUSION

It can bee seen that DFQW has introduced a very promising future in optoelectronics. In fact, development has advanced not only in improving performance, reliability, and integration of existing optical components, but also for cultivating novel optical functions. A planar, compatible OEIC in which a variety of different optical and electronic devices are composed of a common MQW structure, is proposed. It has been demonstrated that this concept is expected to be applicable to long-wavelength materials such as AlInAs/InGaAs and InGaAsP/InP MQW and is believed to focus an important direction of OEIC structure towards high performance and productivity. Another aspect which is of interest will be photonic integrated circuits. Integration of InGaAs/InP MQW laser and a low-loss waveguide in the long-wavelenght region with high coupling efficiency using a cap-on-source-annealing technique has succeeded. This integration technique does not require a re-growth process, and it should prove useful for a variety of integrated devices, including mode-locked lasers and lasers integrated with optical modulators. In the future, further device enhancement and progressions are expected. In addition, wavelength demultiplexing moduator is foreseen as a new area of development.

ACKNOWLEDGEMENT

The author would like to thank Jeanny WC Chan and the OPTO Group at HKU for technical assistance. This work is support by HKU-CRCG grant.

Reference

[1] W. D. Laidig, N. Holonyak, Jr., and M. D. Camras, Appl. Phys. Lett. **38,** 776 (1981)
[2] N. Holonyak, Jr., W. D. Laidig, and M. D. Camras, Appl. Phys. Lett. **39,** 102 (1981)
[3] B.S.Ooi, S.G.Ayling, A.C.Bryce, and J.H.Marsh, IEEE Phot. Tech. Lett. **7,** 944 (1995)
[4] K.Kerkel, J.Oshinowo, A.Forchel, J.Weber, and E.Zielinski, Appl. Phys. Lett. **67,** 3456 (1995)
[5] S.Sudo, H.Onishi, Y.Nakano, Y.Shimogaki, K.Tada, M.J.Mondry, and L.A.Coldren, Jpn. J. Appl. Phys. **35** 1276 (1996)
[6] S.Y.Hu, M.G.Peters, D.B.Young, A.C.Gossard, and L.A.Coldren, Phot. Tech. Lett. **7,** 712 (1995)
[7] P.D.Floyd, B.J.Thibeault, J.Ko, D.B.Young, L.A.Coldren and J.L.Merz., LEOS anneal meeting, 207 (Boston, Nov 1996)
[8] P.J.Poole, M.Davies, M.Dion, Y.Feng, S.Charbonneau, R.D.Goldberg, and I.V.Mitchell, Phot. Tech. Lett. **8,** 1145 (1996)
[9] D. G. Deppe, and N. Holonyak, J. Appl. Phys. **64,** R93 (1988)
[10] B. L. Weiss, Ed., Special Issue, Opt. Quantum. Electron. **23,** S799 (1991)
[11] J. H. Marsh, Semicond. Sci. Technol., **8,** 1136 (1993)
[12] P. Chen and A. J. Steckl, J. Appl. Phys. **77,** 5616 (1995)
[13] I.V.Bradley, W.P.Gillin, K.PHomewood, and R.P.Webb., J. Appl. Phys. **73,** 1686 (1993)
[14] B. L. Weiss, I. V. Bradley, and N. J. Whitehead, J. Appl. Phys. **71,** 5715 (1992)
[15] G. Bacher, D. Tonnies, D. Eisert, and A. Forchel, J. Appl. Phys. **79,** 4368 (1996)
[16] S.J.Lycett, A.J.Dewdney, M.Chisoni, C.E.Norman and R.Murray, J. Elect. Mat. **24,** 197 (1995)
[17] J. E. Epler, R. L. Thornton, and T. L. Paoli, Appl. Phys. Lett. **52,** 1371 (1988)
[18] S.Burkner, M.Maier, E.C.Larkins, W.Rothemund, E.P.O'Reilly, and J.D.Ralston, J. Elec. Mat. **24,** 805 (1995)
[19] S. W. Ryu, I. Kim, and B. D. Choe, Appl. Phys. Lett. **67,** 1417 (1995)

[20] W. C. Shiu, J. Micallef, I. Ng, and E. H. Li, Jnp. J. Appl. Phys. **34,** 1778 (1995)
[21] I.J.Pape, P.LiKamWa, J.P.R.David, P.A.Clazton, P.N.Robson and D.Sykes, Electron. Lett. **24,** 910 (1988)
[22] K. Nakashima, Y. Kawaguchi, Y. Kawamura, Y. Imamura and H. Asahi, Appl. Phys. Lett. **52,** 1383 (1988)
[23] S. A. Schwarz, M. Koza, L. Nazar, and B. J. Skromme, Appl. Phys. Lett. **53,** 1051 (1988)
[24] C. Francis, M. A. Bradley, P. Boucaud, F. H. Julien and M. Razeghi, Appl. Phys. Lett. **62,** 178 (1993)
[25] J. Micallef, E. H. Li, and B. L. Weiss, J. Appl. Phys. **73,** 7524 (1993)
[26] K. Mukai, M. Sugawara, and S. Yamzaki, Phy. Rev. B. **50,** 2273 (1993)
[27] E. H. Li, J. Micallef, and W. C. Shiu, Mat. Res. Soc. Symp. Proc. **417**, 289 (1996)
[28] Y.Chan, W.C.Shiu, W.K.Tsui, and E.H.Li, MRS FALL O8.4 (Boston, Dec 1996)
[29] E. H. Li, B. L. Weiss and K. S. Chan, Phy. Rev. B. **46,** 15181 (1992)
[30] J.Micallef, E.H.Li, K.S.Chan, and B.L.Weiss, Proc SPIE **1675**, 211 (1992)
[31] M.C.Y.Chan, K.S.Chan, and E.H.Li, Proc SPIE **2886**, 140 (1996)
[32] E. H. Li (to be published)
[33] E. H. Li, Appl. Phys. Lett. **69,** 460 (1996)
[34] J.D.Ralston, W.J.Schaff, D.P.Bour, and L.F.Eastman, Appl. Phys. Lett. **54,** 534 (1989)
[35] E. H. Li and W. C. H. Choy, IEEE Phon. Tech. Lett. **7,** 881 (1995)
[36] E. H. Li, B. L. Weiss, K. S. Chan, and J. Micallef, Appl. Phys. Lett. **62,** 550 (1993)
[37] J. Micallef, E. H. Li, and B. L. Weiss, Appl. Phys. Lett. **62,** 3164 (1993)
[38] S. K. Han, S. Sinha, and R. V. Ramaswarmy, Appl. Phys. Lett. **64,** 760 (1994)
[39] S.I.Hansen, J.H.Marsh, J.S.Roberts, and R.Gwilliam, Appl. Phys. Lett. **58,** 1398 (1991)
[40] A. S. W. Lee, and E. H. Li, Appl. Phys. Lett. **69,** 1 (1996)
[41] E. H. Li, and K. S. Chan, Elect. Lett. **29**, 1233 (1993)
[42] S. F. Yu and E. H. Li, IEEE Phot. Tech. Lett. **8,** 482 (1996)
[43] D. Hofstetter, H. P. Azppe, J. E. Epler, and P. Riel, Appl. Phys. Lett. **67**, 1978 (1995)
[44] W. C. H. Choy and E. H. Li, IEEE J. Quantum Elec. **33**, no.3 (1997)
[45] Y. Suzuki, H. Iwamura, T. Miyazawa, and O. Mikami, IEEE J. Quantum Elec. **30,** 1794 (1994)
[46] J. J. He, Y. Feng, E. S. Koteles, P. J. Poole, M. Davies, M. Dion, R. Goldberg, I. Mitchell and S. Charbonneau, Elect. Lett. **31,** 2094 (1995)
[47] A.G.Steele, M.Buchanan, H.C.Liu, and Z.R.Wasilewski, J. Appl. Phys. **75,** 8234 (1994)
[48] Y.Cheng, A.S.W.Lee, and E.H.Li, IEEE TENCON'95, 81 (1995); Y. Cheng, *MPhil Thesis* (University of Hong Kong, 1997)
[49] I. V. Bradley, W. L. Weiss, and J. S. Roberts, Opt. Quantum Elect. **23,** S823 (1991)
[50] Y.T.Oh, S.K.Kim, Y.H.Kim, T.W.Kang, and C.Y.Hong, J. Appl. Phys. **77,** 2415 (1995)
[51] T. E. Schlesinger and T. Kuech, Appl. Phys. Lett. **49,** 519 (1986)
[52] G. P. Kothiyal and P. Bhattacharya, J. Appl. Phys. **63,** 2760 (1988)
[53] S. J. Fancey, G. S. Buller, J. S. Massa, A. C. Walker, C. J. McLean, A. McKee, A. C. Bryce, J. H. Marsh, and R. M. De La Rue, J. Appl. Phys. **79,** 9390 (1996)
[54] E. H. Li and B. L. Weiss, IEEE J. Quantum Elect. **29,** 311 (1993)
[55] E. H. Li, B. L. Weiss, and K. S. Chan, IEEE J. Quantum Elect. **32,** 1399 (1996)
[56] E. H. Li, K. S. Chan B. L. Weiss, and J. Micallef, Appl. Phys. Lettl **63,** 533 (1993)
[57] J. Kuhn, C. Kaden, V. Harle, H. Bolay, F. Scholz, H. Schweizer, H. Hillmer, R. Losch, and W. Schlapp., Nuclear Instru. Meth. Phys. Res. **B106,** 471 (1995)
[58] C.W.Lo, S.F.Yu, and E.H.Li, IEEE Electron Devices Meeting, 30 (Hong Kong, 1995)
[59] E. H. Li, B. L. Weiss, and A. Laszcz, Elect. Lett. **28,** 885 (1992)
[60] J.D.Ralston, M.Ramsteiner, B.Dischler, M.Maier, G.Brandt, P.Koidl, J. Appl. Phys. **70**, 2195 (1991)
[61] P.D.Floyd, M.G.Peters, L.A.Coldren, and J.L.Merz, IEEE Phot. Tech. Lett. **7,** 1388 (1995)